Aeroelastic Loads Predictions using Finite Element Aerodynamics

Jack C. Rowan* and Thomas A. Burns†
Douglas Aircraft Company, Long Beach, Cal.

Aerodynamic and structural influence coefficients are utilized to determine the load distributions, deflections, and trim parameters for a vehicle in quasi-static aeroelastic equilibrium. A matrix formulation is used to solve the various quasi-static aeroelastic problems. Nonlinearities in the aeroelastic trim equations are accounted for by an iteration of the classical closed-form solution. Aerodynamic and structural idealizations are related by a surface spline transformation. Solutions are developed for symmetric, antisymmetric, and asymmetric load conditions on symmetric vehicles of general geometric shapes, which may include both lifting surfaces and lifting bodies.

Nomenclature

a = acceleration vector
b = wing span
C_{mac} = reference chord
ΔC_p = surface box pressure coefficients
f = force
Δh = elastic deflection
M = initial chamber
m = slope
N = load factor
n = unit normal
P = applied load
$\bar{p}$ = position vector relative to center of gravity
q = nondimensional rolling velocity
$\bar{q}$ = dynamic pressure
$\bar{q}$ = nondimensional pitching velocity
r = position vector relative to coordinate origin
$\bar{r}$ = nondimensional yawing velocity
V = velocity
X,Y,Z = Cartesian coordinate system
W = weight
w = normalwash
α = angular displacement about Y axis
β = angular displacement about Z axis
γ = dihedral angle
δ = control surface deflection angle
Δ = structural flexibility coefficient
ξ,η,ζ = coordinates relative to c. g.
θ = initial twist
$\dot{\phi}$ = angular velocity about X axis
λ = trim parameter
μ = body element singularity strength
ω = angular velocity vector

Subscripts

A = antisymmetric
a = aerodynamic (force)
c = concentrated (force)
c.g. = center of gravity
D = displacement grid
F = force grid
I = inertial (force)
K = number of control surfaces
i,j,k = indexes
O = initial value
ref. = reference
S = symmetric
x,y,z = coordinate directions
rcf = number of concentrated forces

Superscripts

T = matrix transpose
-1 = matrix inversion

Presented as Paper 74-106 at the AIAA 12th Aerospace Sciences Meeting, Washington, D. C., January 30-February 1, 1974; submitted February 11, 1974; revision received February 26, 1975.

Index categories: Aircraft Aerodynamics (including Component Aerodynamics); Aircraft Structural Design (including loads).

*Principal Engineer, Structural Mechanics Section. Member AIAA.
†Senior Engineer Scientist, Structural Mechanics Section.

Introduction

THE use of large-order matrix solutions for the analysis of complex structures has created a need for a complementary approach to the external loads problem. Finite element structural analysis techniques demand that the external loads be distributed over the structure at discrete points. Therefore, shear, moment, and torque distributions along a pseudoelastic axis are no longer sufficient to define the external load distributions required by the stress analysis. A general finite element approach to the problem of the determination of aeroelastic loads on a flexible vehicle flying in a state of quasi-static equilibrium is presented here. Structural and aerodynamic influence coefficients obtained from finite element idealizations of the aircraft are utilized as a basis for the method.

The technique is primarily an extension of the method first suggested by Hedman[1] and later generalized by Rodden [2]. It is naturally similar to such large-scale analysis capabilities as the Boeing-NASA FLEXTAB System[3] and the works of Roskam[4] and Kemp,[5] which are primarily concerned with the determination of the stability characteristics of elastic airplanes. This work extends the efforts of the aforementioned authors by including the effects of drag and certain nonlinear parameters and detailing a solution for nonplanar geometries.

The aerodynamic technique used is the Doublet-Lattice Method (DLM) and Method of Images. This lifting surface theory, suggested by Hedman and expanded by Giesing, Kalman,and Rodden[6] as an approach to various steady and unsteady aerodynamic problems, provides a very powerful tool for determination of aerodynamic influence coefficients (AIC). James[7] remarks on the accuracy of this method. Stahl et al.[8] suggested the use of second-order airfoil chordwise chambering as an approximation to the chordwise flexure mode of a high aspect ratio swept wing. A surface spline technique has been used to generalize this concept to n^{th} order cambering both chordwise and spanwise. This method was suggested by Harder and Desmarais[9] and provides a single-step interpolation matrix which relates the aerodynamic and structural idealizations.

The method accounts for certain nonlinearities by an iteration of the classical closed-form linear static aeroelastic solution. Using this approach the effects of drag and inertial coupling may be included within the aeroelastic trim solution. The equations are cast in symmetric and antisymmetric form and three selected trim scalars are determined for each case. Unsymmetric conditions are obtained by linear combinations of symmetric and antisymmetric conditions. The trim scalars to be solved for are determined by the user.

General Concepts and Definitions

The following derivation is for flight vehicles with geometric symmetry. A Cartesian coordinate system attached to the vehicle with $Y=0$ on the plane of symmetry is used as shown in Fig. 1. Because of symmetry, only half the airplane is analyzed.

Matrices of influence coefficients for elastic structural deflections, aerodynamic forces, inertial forces, and applied forces are used to solve for the external loads, elastic deflections, and trim parameters. The AIC's and SIC's (structural influence coefficients) may be determined theoretically or empirically. Inertial force influence coefficients are readily calculated from mass distribution data and applied force influence coefficients are defined by the engineer.

Aerodynamic and structural finite element idealizations of aircraft are required to determine theoretical influence coefficients for the aeroelastic analysis. Aerodynamically, the vehicle is idealized as a combination of lifting bodies and lifting surfaces. Forces normal and lateral to the body axis are developed by lifting bodies, and forces normal to the surface are developed by lifting surfaces. Structurally, the vehicle is idealized as bars and panels, as in the force or displacement methods of structural analysis. Three orthogonal load (or deflection) vectors must be defined at a number of joints sufficient to predict the elastic behavior of the aircraft. For lifting surface structure, the vectors are assumed to be normal and tangen to the local surface reference plane and, for lifting body structure, the vectors are assumed to be in the X,Y, and Z coordinate directions.

These two idealizations lead to two separate and independent finite element grid systems. The force point grid consists of the points at which aerodynamic forces are calculated plus any additional points required to define the application of concentrated forces (thrust, landing gear loads, etc.) or concentrated weights. The displacement grid consists of the points at which elastic deflections used in the aeroelastic analysis are determined plus the concentrated force and weight points. The displacement grid is related to the force grid by a surface spline transformation matrix

Aerodynamic Influence Coefficients

The aerodynamic influence coefficients relate rigid body modes and elastic deflection modes to lift forces in the Y and Z directions on lifting bodies and to lift forces normal to lifting surfaces. These coefficients are determined by subdividing the lifting surfaces and bodies into a finite number of aerodynamic elements. One or more flow singularities are applied on each element in order to create a flowfield with prescribed normal velocity (normalwash) at selected control points. The normalwashes must create a flow tangent to the surface at the control points. If the number of control points equals the number of flow singularities, the system of equations relating singularity strengths to normalwashes is determinate and the strengths giving specified normalwashes may be calculated. Lift forces are then calculated from the singularity strengths.

To discuss the calculation of the AIC matrices, it is necessary to refer to a specific aerodynamic theory. The doublet-lattice method and the method of images developed by Giesing, Kalman, and Rodden[6] will be used here. This theory is for subsonic unsteady aerodynamics, but only the steady-flow portion will be outlined here. Since the doublet-lattice method is well documented[1,6-8] emphasis here will be placed on determining the boundary conditions peculiar to quasi-static aeroelastic analysis.

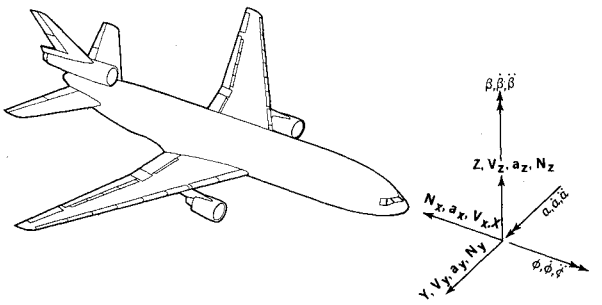

Fig. 1 Coordinate system.

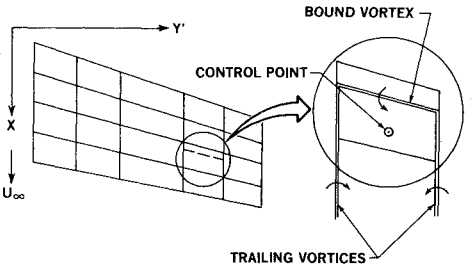

Fig. 2 Horseshoe vortex system.

In the doublet-lattice and image method, the airplane is idealized as a combination of lifting surfaces and lifting bodies. Lifting surfaces are divided into trapezoidal elements (boxes) arranged in strips parallel to the freestream so that surface edges, fold lines, and hinge lines lie on box boundaries. For steady flow a horsehoe vortex is placed on each box such that the bound vortex coincides with the quarter-chord line of the box (Fig. 2). The surface boundary condition is a prescribed normalwash (wash in Z′ direction divided by the freestream velocity) at the control point of each box. The box control point is centered spanwise on the three-quarter-chord line of the box.

Lifting bodies are idealized as cylinders with elliptic cross sections. The axis of an idealized body is parallel to the X-axis. The idealized body is divided into chordwise segments; two such divisions are made: one for slender body elements and one for interference elements. The boundary condition for lifting bodies is specified normalized upwash and sidewash at the midpoint of the longitudinal axis for each element.

Slender body theory based on axial singularities is used to simulate the effect of isolated bodies. For circular cross sections the axial singularity is simply a line doublet on the element axis. Since sidewash as well as upwash are to be satisfied, there are two axial singularities used on each slender body element. The singularity strengths for a slender body element μ_{oy} and μ_{oz} are functions of the local cross section and local sidewash or upwash.

To divert the flow around a body that is in the presence of a lifting surface, an image of each horseshoe vortex on the surface that is within the longitudinal range of the body is generated within the body. The cross section of the body is constant for the image system. The image horseshoe vortex has the same strength as the corresponding surface vortex. For bodies with elliptic cross sections, the image is developed in the same manner by using the circle determined by the radius and center of curvature of the point on the body surface nearest the surface vortex system. Images not in the same quadrant as the corresponding surface vortices are neglected.

The image system is the primary means for adjusting the flowfield around bodies in the presence of lifting surfaces.

However, due to three-dimensional effects, i.e., the trailers do not extend from infinity to infinity and the bound vortices are not canceled by their images, etc., it is not completely effective in doing this and a residual flow must be added. The residual flow is generated by the same type of axial singularities as used for slender body theory. Each body is divided into interference elements analogous to slender body elements except that the elements have the cross section used for the image system. The normalwashes due to lifting surface vortices and their images are then calculated at various meridian angles.

The basic aerodynamic equation relating singularity strengths to total normalwash is

$$\left\{ \begin{array}{c} \mu_y \\ \hline \Delta C_p \\ \hline \mu_z \end{array} \right\} = [D_T]^{-1}\{w\} \tag{1}$$

Where D_T = downwash influence coefficient matrix and w = normalwash boundary condition. The lift forces are determined from the known singularity strengths by integrating the body pressure field and multiplying the surface elements by their respective areas

$$\{FAL\} = q[BFS] \left\{ \begin{array}{c} \mu_y \\ \hline \Delta C_p \\ \hline \mu_z \end{array} \right\} \tag{2}$$

where [BFS] = body pressure field integration matrix.

Now the lift at the force points may be determined from the normalwashes at the control points by substituting Eq. (l) in Eq. (2) (half the total lift force is calculated at points on the plane of symmetry). Of course, if the pressure distributions on the vehicle are not desired, the lift forces may be obtained directly from the singularity strengths.

$$\{FAL\} = q[BFS][D_T]^{-1}\{w\} \tag{3}$$

The aerodynamic solution may include the effect of images for symmetry or antisymmetry about the plane of symmetry and/or the ground plane.

The lift forces due to rigid body modes, {FRALS} and {FRALA}, and the corresponding AIC matrices, [FALUS] and [FALUA], may now be calculated by obtaining the normalwashes for these modes (the final S or A in matrix names indicates symmetry or antisymmetry, respectively). There are three types of rigid body modes: initial configuration, rigid body motion, and control surface deflection.

The initial configuration mode is the initial or built-in twist and camber of the lifting surfaces and bodies. Since this analysis is restricted to aircraft with geometric symmetry, the normalwash for the initial configuration mode $\{w_{OS}\}$ is necessarily symmetric. The normalwash for the rigid body motion mode is equal to the component of the control point velocity normal to the surface (or body) divided by the freestream velocity,

$$w_{RB_i} = \mathbf{V}_i \cdot \mathbf{n}_i / V_\infty$$

The velocity of the i^{th} control point is

$$\mathbf{V}_i = \mathbf{V}_{c.g.} + \boldsymbol{\omega} \times \mathbf{P}_i$$

where vectors $\boldsymbol{\omega}$ and $\mathbf{P}_i$ are defined in Fig. 3 and Eq. (20).

The control surface deflection modes are obtained by specifying the normalwash on the control surface elements. Control surface deflections are defined as positive when the angle of attack on the control surface is increased. The downwash at any control point on the j^{th} control surface due to the

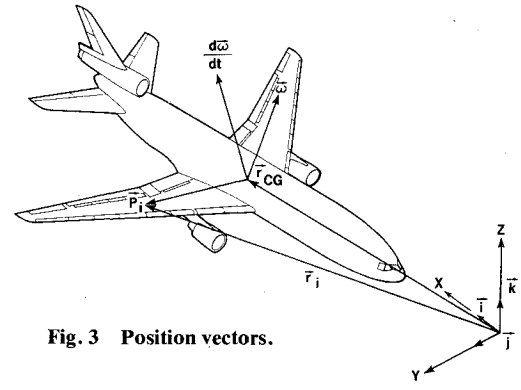

Fig. 3 Position vectors.

angular deflection δ_j is $V_\infty \tan \delta_j$. Since the normalwash is defined positive in the Z′ direction, the normalwash at any point on the control surface is

$$w = -V_\infty \tan \delta_j / V_\infty = -\delta_j$$

using small angle theory.

The nondimensional angular velocity parameters are

$$\bar{p} = \dot{\phi} b / 2V_\infty, \quad \bar{q} = \dot{\alpha} C_{mac} / 2V_\infty, \quad \bar{r} = \dot{\beta} b / 2V_\infty$$

The symmetric and antisymmetric normalwashes due to rigid body modes are

$$\{w_{RS}\} = \{w_{OS}\} + \{w_{RBS}\} + \{w_{\delta_S}\} = [WUNITS]\,[\overline{KULS}]\,\{\overline{\lambda_{AS}}\} \tag{4a}$$

$$\{w_{RA}\} = \{w_{RBA}\} + \{w_{\delta_A}\} = [WUNITA]\,[\overline{KULA}]\,\{\overline{\lambda_{AA}}\} \tag{4b}$$

where

$$[WUNITS] = \left[\begin{array}{c|c|c|c} \theta_{z_{o_i}} & M_{z_{o_i}} & 0 & 0 \\ \hline -\theta_{y'_{o_i}} & -M_{y'_{o_i}} & -\cos\gamma_i & -\frac{2}{C_{MAC}}\{\bar{X}_i \cos\gamma_i\} \\ \hline -\theta_{y_{o_i}} & -M_{y_{o_i}} & -1\text{'s} & -\frac{2}{C_{MAC}}\{\bar{X}_i\} \end{array} \right] [WCSS]$$

$$[WUNITA] = \left[\begin{array}{c|c|c} 1\text{'s} & \frac{2}{b}\{\bar{X}_i\} & \frac{2}{b}\{\bar{Z}_i\} \\ \hline -\sin\gamma_i & -\frac{2}{b}\{\bar{X}_i \sin\gamma_i\} & -\frac{2}{b}\{\bar{Z}_i \sin\gamma_i + \bar{Y}_i \cos\gamma_i\} \\ \hline 0 & 0 & -\frac{2}{b}\{\bar{Y}_i\} \end{array} \right] [WCSA]$$

$(\bar{X}_i, \bar{Y}_i, \bar{Z}_i)$ are the coordinates of the i^{th} control point relative to the aerodynamic reference point $(X_{ref}, Y_{ref}, Z_{ref})$.

The j^{th} column of [WCSS] or [WCSA] has −1's in the rows corresponding the elements on the j^{th} symmetric and antisymmetric control surface. All other elements equal zero.

$$[\overline{KULS}] = \left[\begin{array}{c|c|c|c|c} 1 & 0 & 0 & 0 & \\ 1 & 0 & 0 & 0 & \\ 0 & 1 & a & c & \\ 0 & 0 & 1 & 0 & \\ \hline & & & & I \end{array} \right]; \quad [\overline{KULA}] = \left[\begin{array}{c|c|c|c} 1 & d & e & \\ 0 & 1 & 0 & \\ 0 & 0 & 1 & \\ \hline & & & I \end{array} \right]$$

$$a = (2/C_{mac})(X_{ref} - X_{c.g.}) \qquad c = (2/b)(Y_{ref} - Y_{c.g.})$$

$$d = (2/b)(X_{ref} - X_{c.g.}) \qquad e = (2/b)(Z_{ref} - Z_{c.g.})$$

and the aerodynamic trim parameters are

$$\{\overline{\lambda_{a_S}}\} = [1.0, \alpha, \bar{q}, \bar{p}, \delta_{S_1}, \ldots, \delta_{S_{KS}}]^T$$

$$\{\overline{\lambda_{a_A}}\} = [\beta, \bar{r}, \bar{p}, \delta_{A_1}, \ldots, \delta_{A_{KA}}]^T$$

Now the symmetric and antisymmetric lift forces due to rigid body modes can be obtained by substituting Eq. (4) in Eq. (3)

$$\{FRALS\} = q\,[BFSS]\,[DTS]^{-1}\,[WUNITS]\,[\overline{KULS}]\{\overline{\lambda_{AS}}\} \quad (5a)$$

$$\{FRALA\} = q\,[BFSA]\,[DTA]^{-1}\,[WUNITA]\,[\overline{KULA}]\{\overline{\lambda_{AA}}\} \quad (5b)$$

Therefore, the AIC matrices for rigid body modes are

$$[FALUS] = [BFSS]\,[DTS]^{-1}\,[WUNITS] \quad (6a)$$

$$[FALUA] = [BFSA]\,[DTA]^{-1}\,[WUNITA] \quad (6b)$$

The [BFS] and [DT] matrices vary with Mach number due to the Prandtl-Glauert transformation.

The lift forces due to elastic deflection modes, $\{FELAS\}$ and $\{FELAA\}$, and the corresponding AIC matrices [AICS] and [AICA], are analogously calculated by determining the normalwashes for the elastic modes. The slope at each control point $m_i = (dz'/dx)_i$ for any elastic mode $\{\Delta h\}$ is calculated by the surface spine matrix [WSS]

$$\{m_i\} = [WSS]\{\Delta h\} \quad (7)$$

From Eqs. (3) and (7), the lift forces due to elastic deflections are

$$\{FELAS\} = q\,[BFSS]\,[DTS]^{-1}\,[WSS]\{\Delta h_S\} \quad (8a)$$

$$\{FELAA\} = q\,[BFSA]\,[DTA]^{-1}\,[WSS]\{\Delta h_A\} \quad (8b)$$

Therefore the AIC matrices for elastic deflections are

$$[AICS] = [BFSS]\,[DTS]^{-1}\,[WSS] \quad (9a)$$

$$[AICA] = [BFSA]\,[DTA]^{-1}\,[WSS] \quad (9b)$$

The surface spline matrix [WSS] is a function of geometry only. Therefore, for a given idealization and a specified ground effect, [AICS] and [AICA] vary only with Mach number.

Structural Influence Coefficients

The SIC matrix required in this analysis relates the forces at the force points to the elastic deflections at the displacement points. This matrix is obtained from the matrix of SIC's (also commonly called "flexibility influence coefficients") for forces and displacements on the structural grid, [Δ], by utilizing the surface spline transformation matrix.

In general, [Δ] will include some influence coefficients not required for the aeroelastic analysis. Also, the sort may not be that required by the AIC's or the spline transformation matrix. Deflections lateral to lifting bodies and normal to lifting surfaces and lifting bodies due to forces in the local coordinate directions at each displacement point are extracted from [Δ] by

$$[\Delta R] = [CDELTA]^T\,[\Delta]\,[CFS\O RT] \quad (10)$$

where [CDELTA] is a deflection extractor and [CFSØRT] is a force extractor.

Matrix [ΔR] is related to forces on the force point grid by a surface spline transformation matrix. This transformation matrix relates the displacements at the displacement points, $\{h'_D\}$, to the displacements at the force points, $\{h'_F\}$, by

$$\{h'_F\} = [Z]\{h'_D\} \quad (11)$$

where the primes denote that the displacements are normal to the local surface.

The forces at the displacement points $\{f'_D\}$ that are statically equivalent to the forces at the force points, $\{f'_F\}$, may be determined by using Eq. (11) and the fact that the work done by each set of forces must be equal.

$$\{f'_D\} = [Z]^T\{f'_F\} \quad (12)$$

The elastic deflections lateral to lifting bodies and normal to lifting surfaces and lifting bodies at the displacement points are

$$\{\Delta h\} = [\Delta R]\{f'_D\} = [\Delta R]\,[Z]^T\{f'_F\} = [SIC]\{f'_F\} \quad (13)$$

Therefore, in terms of the symmetric and antisymmetric SIC matrices on the structural grid, $[\Delta_S]$ and $[\Delta_A]$, respectively, the SIC matrices required for the aeroelastic analysis are

$$[SICS] = [CDELTA]^T\,[\Delta_S]\,[CFS\O RT]\,[Z]^T \quad (14a)$$

$$[SICA] = [CDELTA]^T\,[\Delta_A]\,[CFS\O RT]\,[Z]^T \quad (14b)$$

Surface Spline

The Harder[9] spline is based on symmetrically loaded plates and relates the displacements on the displacement grid to applied loads by

$$\{h'_D\} = [KD]\{C\} \quad (15)$$

The elements of [KD] are functions of the coordinates of the displacement points. A similar matrix, [KF], that is a function of force grid and displacement grid coordinates relates deflections on the force grid to loads on the displacement grid by

$$\{h'_F\} = [KF]\{C\} = [KF]\,[KD]^{-1}\{h'_D\} \quad (16)$$

Similarly, slopes at the aero control points are calculated by

$$\{m\} = [DKFDX]\,[KD]^{-1}\{h'_D\} \quad (17)$$

where

$$[DKFDX] = (\partial/\partial x)\,[\overline{KF}]$$

and $[\overline{KF}]$ is analogous to [KF] except that control points are used in lieu of aero force points.

Since an airplane is made up of various lifting surfaces and bodies, it is necessary to separate the force and displacement points into groups such that each group lies in a region that may be approximated by a surface spline. Any such region is called a "superpanel". Summing the effects of the nsp superpanels and the nonlifting points, the surface spline matrix [Z] is

$$[Z] = [ZCF] + \sum_{j=1}^{nsp} ([RZ]_j\,[KF]_j\,[KD]_j^{-1}\,[CZ]_j) \quad (18)$$

where [ZCF] = matrix extracting deflections at nonlifting displacement points and [RZ] and [CZ] are extractor matrices. Similarly, the differential surface spline matrix [WSS] is

$$[WSS] = \sum_{K=1}^{2} ([RDH]_K\,[WR]\,[CDH]_K)$$

$$[WR] = \sum_{j=1}^{nsp} ([RZ]_j\,[DKFDX]_j\,[KD]_j^{-1}\,[CZ]_j) \quad (19)$$

and $[RDH]_1$, $[RDH]_2$, $[CDH]_1$, and $[CDH]_2$ are row and column extractors.

Inertial and Applied Force Influence Coefficients

The inertial force at a point is defined as the negative of the product of the mass acting at that point and the acceleration of the point. The applied force at a point refers here to a concentrated external load applied to the vehicle such as thrust or a landing gear load. The magnitudes of the applied forces are trim parameters and, as such, may be specified or solved for in each loading condition. The influence coefficients for inertial and applied forces are derived using the rigid body geometry. That is, changes in the position of the points of application or directions of these forces due to elastic deflections are ignored.

In order to calculate the acceleration of the i^{th} point, the following vectors are defined (Fig. 3)

$$\mathbf{r}_{c.g.} = X_{c.g.}\mathbf{i} + Y_{c.g.}\mathbf{j} + Z_{c.g.}\mathbf{k} =$$
position vector of c.g.

$$\mathbf{r}_i = X_i\mathbf{i} + Y_i\mathbf{j} + Z_i\mathbf{k} =$$
position vector of i^{th} force point

$$\boldsymbol{\omega} = -\dot{\phi}\mathbf{i} + \dot{\alpha}\mathbf{j} + \dot{\beta}\mathbf{k} =$$
airplane angular velocity about c.g.

$$d\boldsymbol{\omega}/dt = -\ddot{\phi}\mathbf{i} + \ddot{\alpha}\mathbf{j} + \ddot{\beta}\mathbf{k} =$$
airplane angular acceleration about c.g.

$$\mathbf{a}_{c.g.} = a_{x_{c.g.}}\mathbf{i} + a_{y_{c.g.}}\mathbf{j} + a_{z_{c.g.}}\mathbf{k} =$$
translational acceleration of c.g.

The position vector of the i^{th} force point relative to the c.g. is

$$\mathbf{P}_i = \mathbf{r}_i - \mathbf{r}_{c.g.} = \xi_i\mathbf{i} + \eta_i\mathbf{j} + \zeta_i\mathbf{k} \tag{20}$$

The total acceleration of the i^{th} point is

$$\mathbf{a}_i = \mathbf{a}_{c.g.} + \boldsymbol{\omega} \times (\boldsymbol{\omega} \times \mathbf{P}_i) + d\boldsymbol{\omega}/dt \times \mathbf{P}_i$$

Now, by substituting the nondimensional angular velocity parameters and introducting the airplane load factors, the symmetric and antisymmetric inertia forces are

$$\{f_{IS}\} = -\frac{1}{g}\left[\lceil W_S \rfloor\,[KIS] + \lceil W_A \rfloor\,[KIA]\right][KV]\{\lambda_I\}$$

$$\{f_{IA}\} = -\frac{1}{g}\left[\lceil W_S \rfloor\,[KIA] + \lceil W_A \rfloor\,[KIS]\right][KV]\{\lambda_I\}$$

where

$$[KV] = \begin{bmatrix} I & \\ & V_\infty^2 \end{bmatrix}$$

; $\lceil W_S \rfloor$ and $\lceil W_A \rfloor$ = Weight Matrices

$$[KIS] = \begin{array}{c} \\ nf \\ 2nf \\ 3nf \end{array} \begin{bmatrix} (N_x) & (N_z) & (\ddot{\alpha}) & (N_y) & (\ddot{\phi}) & (\ddot{\beta}) & (\bar{p}^2) & (\bar{q}^2) & (\bar{r}^2) & (\bar{p}\bar{q}) & (\bar{q}\bar{r}) & (\bar{p}\bar{r}) \\ g\{1'_s\} & & \{Z_i - Z_{cg}\} & & Y_{cg}\{1'_s\} & & & \frac{-4}{C_{mac}^2}\{X_i - X_{cg}\} & \frac{-4}{b^2}\{X_i - X_{cg}\} & \frac{4Y_{cg}}{bC_{mac}}\{1'_s\} & & \frac{-4}{b^2}\{Z_i - Z_{cg}\} \\ & & & & & & \frac{-4}{b^2}\{Y_i\} & & \frac{-4}{b^2}\{Y_i\} & & & \\ & g\{1'_s\} & -\{X_i - X_{cg}\} & & Y_{cg}\{1'_s\} & & \frac{-4}{b^2}\{Z_i - Z_{cg}\} & \frac{-4}{C_{mac}^2}\{Z_i - Z_{cg}\} & & & \frac{-4Y_{cg}}{bC_{mac}}\{1'_s\} & \frac{-4}{b^2}\{X_i - X_{cg}\} \end{bmatrix}_{12}$$

$$[KIA] = \begin{array}{c} \\ nf \\ 2nf \\ 3nf \end{array} \begin{bmatrix} (N_x) & (N_z) & (\ddot{\alpha}) & (N_y) & (\ddot{\phi}) & (\ddot{\beta}) & (\bar{p}^2) & (\bar{q}^2) & (\bar{r}^2) & (\bar{p}\bar{q}) & (\bar{q}\bar{r}) & (\bar{p}\bar{r}) \\ & & & & & -\{Y_i\} & & & & \frac{-4}{bC_{mac}}\{Y_i\} & & \\ & & & g\{1'_s\} & \{Z_i - Z_{cg}\} & \{X_i - X_{cg}\} & \frac{4Y_{cg}}{b^2}\{1'_s\} & & \frac{4Y_{cg}}{b^2}\{1'_s\} & \frac{-4}{bC_{mac}}\{X_i - X_{cg}\} & \frac{4}{bC_{mac}}\{Z_i - Z_{cg}\} & \\ & & & & -\{Y_i\} & & & & & & \frac{4}{bC_{mac}}\{Y_i\} & \end{bmatrix}_{12} \tag{21}$$

and $\{\lambda_I\}$ is the column matrix of inertial trim parameters given across the top of [KIS] and [KIA].

By adding a set of concentrated applied forces to the preceding equations, the final inertial and applied force equations become

$$\{f_{cs}\} + \{f_{IS}\} = [\overline{FCILS}]\begin{Bmatrix}\lambda_{cs}\\ \lambda_I\end{Bmatrix} \; ; \; \{f_{ca}\} + \{f_{IA}\} = [\overline{FCILA}]\begin{Bmatrix}\lambda_{ca}\\ \lambda_I\end{Bmatrix} \tag{22}$$

where

$$[\overline{FCILS}] = {}_{3nf}\left[\{f_{ps}\} \mid [FCLAMS] \mid -\left[\frac{1}{g}\left[\lceil W_S \rfloor\,[KIS] + \lceil W_A \rfloor\,[KIA]\right][KV]\right]\right]$$

$$[\overline{FCILA}] = {}_{3nf}\left[\{f_{pa}\} \mid [FCLAMA] \mid -\frac{1}{g}\left[\lceil W_S \rfloor\,[KIA] + \lceil W_A \rfloor\,[KIS]\right][KV]\right]$$

and $\{\lambda_{cs}\}$ and $\{\lambda_{ca}\}$ are applied force trim parameters. Matrices $\{f_{ps}\}$ and $\{f_{pa}\}$ are catchall force arrays for including any special loads such as external stores. The j^{th} column of [FCLAMS] or [FCLAMA] contains the X, Y, and Z force components for unit P_{S_j} or P_{A_j}, respectively.

Trim Solution

For a given set of trim parameters, $\{\lambda_S\}$ and $\{\lambda_A\}$, there are two aeroelastic matrix equations: one relates the elastic deflections to the net forces; the other relates the net forces to the elastic deflections. Aerodynamic drag forces and the squares and cross products of angular velocities are nonlinear and are calculated by an iterative solution of the equilibrium equations

$$\{\lambda_S\} = \begin{Bmatrix} \bar{\lambda}_{AA} \\ \hline \lambda_{ca} \\ \hline \lambda_I \end{Bmatrix} = \Big[1.0, \alpha, \bar{q}, \bar{p}, \delta_{S_1}, \ldots, \delta_{S_{KS}}, 1.0, P_{S_1}, \ldots, P_{S_{rcfS}}, N_x, N_z, \ddot{\alpha}, N_y, \ddot{\phi}, \ddot{\beta}, \bar{p}^2, \bar{q}^2, \bar{r}^2, \overline{pq}, \overline{qr}, \overline{pr}\Big]^T$$

$$\{\lambda_A\} = \begin{Bmatrix} \bar{\lambda}_{AS} \\ \hline \lambda_{cs} \\ \hline \lambda_I \end{Bmatrix} = \Big[\beta, \bar{r}, \bar{p}, \delta_{A_1}, \ldots, \delta_{A_{KA}}, 1.0, P_{A_1}, \ldots, P_{A_{rcfA}}, N_x, N_z, \ddot{\alpha}, N_y, \ddot{\phi}, \ddot{\beta}, \bar{p}^2, \bar{q}^2, \bar{r}^2, \overline{pq}, \overline{qr}, \overline{pr}\Big]^T$$

The local aerodynamic lift forces are the sum of the lift forces due to rigid body modes and elastic deflections.

$$\{f_{aL_S}\} = q[FALUS]\,[KULS]\,\{\lambda_S\} + q[AICS]\{\Delta h_s\} \quad (23a)$$

$$\{f_{aL_A}\} = q[FALUA]\,[KULA]\,\{\lambda_A\} + q[AICA]\,\{\Delta h_A\} \quad (23b)$$

The full aerodynamic force array in the body coordinate system may now be written as the sum of the transformed local aerodynamic lift forces and the iteratively determined drag forces.

$$\{f_{a_S}\} = [RLF]^T\{f_{aL_S}\} + [RX]^T\{f_{aX_S}\} \quad (24a)$$

$$\{f_{a_A}\} = [RLF]^T\{f_{aL_A}\} + [RX]^T\{f_{aX_A}\} \quad (24b)$$

where $[RLF] = [RL]\,[TFF]$, $[RL]$ = local lift force extractor, $[TFF]$ = local lift force rotation matrix, and $[RX]$ = drag force row extractor. The net forces are the sum of the aerodynamic, applied, and inertial forces

$$\{f_S\} = \{f_{a_S}\} + \{f_{C_S}\} + \{f_{I_S}\} \quad (25a)$$

$$\{f_A\} = \{f_{a_A}\} + \{f_{C_A}\} + \{f_{I_A}\} \quad (25b)$$

The elastic deflections are determined from the net forces by

$$\{\Delta h_S\} = [SICS]\,[TFF]\,\{f_S\}, \quad \{\Delta h_A\} = [SICA]\,[TFF]\,\{f_A\} \quad (26)$$

Substituting Eqs. (22-24) into Eq. (25):

$$\{f_S\} = \left[q\,[RLF]^T\,[FALUS]\,[KULS] + [FCILS]\right]\{\lambda_S\} + q\,[RLF]^T\,[AICS]\{\Delta h_S\} + [RX]^T\{f_{aX_S}\} \quad (27a)$$

$$\{f_A\} = \left[q\,[RLF]^T\,[FALUA]\,[KULA] + [FCILA]\right]\{\lambda_A\} + q\,[RLF]^T\,[AICA]\{\Delta h_A\} + [RX]^T\{f_{aX_A}\} \quad (27b)$$

Equations (26) and (27) are the basic static aeroelastic equations. Substituting Eq. (27) into Eq. (26) determines the elastic deflections in terms of known quantities

$$\{\Delta h_S\} = [G_S]^{-1}\,[SICS]\,[TFF]\,\{f_{R_S}\} \quad (28a)$$

$$\{\Delta h_A\} = [G_A]^{-1}\,[SICA]\,[TFF]\,\{f_{R_A}\} \quad (28b)$$

where

$$[G_S] = [I] - q\,[SICS]\,[RL]^T\,[AICS]$$

$$[G_A] = [I] - q\,[SICA]\,[RL]^T\,[AICA]$$

and $\{f_{R_S}\}$, $\{f_{R_A}\}$ are the rigid solution net forces

$$\{f_{R_S}\} = \left[q\,[RLF]^T\,[FALUS]\,[KULS] + [FCILS]\right]\{\lambda_S\} + [RX]^T\{f_{aX_S}\} \quad (29a)$$

$$\{f_{R_A}\} = \left[q\,[RLF]^T\,[FALUA]\,[KULA] + [FCILA]\right]\{\lambda_A\} + [RX]^T\{f_{aX_A}\} \quad (29b)$$

The dynamic pressure at which divergence occurs is readily obtained from Eqs. (28). Since the symmetric elastic deflections become infinite if $|G_S| = 0$, the eigenvalues of

$$[D_S] = [SICS]\,[RL]^T\,[AICS]$$

are the reciprocals of the dynamic pressures at which divergence occurs for a symmetric loading. Hence, divergence occurs at the dynamic pressure equal to the reciprocal of the largest positive real eigenvalue of $[D_S]$. An analogous argument holds for antisymmetric loadings. The associated eigenvectors provide a description of the mode of divergence.

Since the lift forces are required in order to calculate the drag forces, it is necessary to determine the aerodynamic lift forces explicitly

$$\{f_{aL_S}\} = \left[[FRLS] + [FELS]\right]\{\lambda_S\} + [AGINVS]\,[SICS]\,[RX]^T\{f_{aX_S}\} \quad (30a)$$

$$\{f_{aL_A}\} = \left[[FRLA] + [FELA]\right]\{\lambda_A\} + [AGINVA]\,[SICA]\,[RX]^T\{f_{aX_A}\} \quad (30b)$$

where

$[FELS] = [AGINVS]\left[[SICS]\,[RL]^T\,[FRLS] + [SICS]\,[TFF]\,[FCILS]\right]$

$[FELA] = [AGINVA]\left[[SICA]\,[RL]^T\,[FRLA] + [SICA]\,[TFF]\,[FCILA]\right]$

$[FRLS] = q\,[FALUS]\,[KULS]$

$[FRLA] = q\,[FALUA]\,[KULA]$

$[AGINVS] = q\,[AICS]\,[GS]^{-1}$

$[AGINVA] = q\,[AICA]\,[GA]^{-1}$

The symmetric and antisymmetric equilibrium conditions may now be introduced.

$$[CST]^T\{f_S\} = \begin{Bmatrix} \Sigma f_x \\ \Sigma f_z \\ \Sigma M_y \end{Bmatrix} = 0 \;; [CAT]^T\{f_A\} = \begin{Bmatrix} \Sigma f_y \\ \Sigma M_x \\ \Sigma M_z \end{Bmatrix} = 0 \quad (31)$$

Therefore

$$[QLS]\{\lambda_S\} + [QAXST]^T\{f_{aX_S}\} = 0 \quad (32a)$$

$$[QLA]\{\lambda_A\} + [QAXAT]^T\{f_{aX_A}\} = 0 \quad (32b)$$

where

$[QLS] = [RLFCST]^T\left([FRLS] + [FELS]\right) + [CST]^T\,[FCILS]$

$[QLA] = [RLFCAT]^T\left([FRLA] + [FELA]\right) + [CAT]^T\,[FCILA]$

$[RLFCST] = [RLF]\,[CST]$

$[RLFCAT] = [RLF]\,[CAT]$

$[QAXST]^T = [RLFCST]^T\,[AGINVS]\,[SICS]\,[RX]^T + [CST]^T\,[RX]^T$

$[QAXAT]^T = [RLFCAT]^T\,[AGINVA]\,[SICA]\,[RX]^T + [CAT]^T\,[RX]^T$

Three unknowns in $\{\lambda_S\}$ and three unknowns in $\{\lambda_A\}$ are determined by the trim equations. The symmetric and antisymmetric unknown trim parameters are denoted by $\{\lambda_{XS}\}$ and $\{\lambda_{XA}\}$. The columns of [QLS] and [QLA] that are coefficients of $\{\lambda_{XS}\}$ and $\{\lambda_{XA}\}$ are extracted by matrices [CLXS] and [CLXA], respectively. The nonlinear angular velocity parameters are treated as known quantities in Eq. (32). The coefficients of the known trim parameters are extracted from [QLS] and [QLA] by [CLS] and [CLA], respectively. Hence, [CLS] and [CLA] are partial identity matrices having unity on their diagonals except for the columns corresponding to the unknown parameters

The equilibrium Eqs. (32) for the unknown trim parameters are solved

$$\{\lambda_{XS}\} = \left[[QLS]\,[CLXS]\right]^{-1}\left\{[QLS]\,[CLS]\{\lambda_S\} + [QAXST]^T\{f_{aX_S}\}\right\}$$

$$\{\lambda_{XA}\} = \left[[QLA]\,[CLXA]\right]^{-1}\left\{[QLA]\,[CLA]\{\lambda_A\} + [QAXAT]^T\{f_{aX_A}\}\right\}$$

The inverse of [(QLS) (CLXS)] or [(QLA) (CLXA)] exists if the trim parameters selected as unknowns are capable of balancing the vehicle in the symmetric or antisymmetric degrees of freedom, respectively.

To solve for the unknown trim parameters, it is necessary to determine $\{f_{aX_S}\}$, $\{f_{aX_A}\}$, and the unknown nonlinear angular velocities (if any) by iteration. Since both rigid and elastic solutions are often required, and since the rigid solution requires much less computation than the elastic

solution, two separate iterations may be performed. First, the rigid solution may be obtained, then the rigid solution trim parameters and drag forces can be used as initial values for elastic iteration.

The symmetrical and antisymmetrical aeroelastic trimmed force distributions are now determinable by using Eqs. (27-29). Unsymmetrical loadings may be developed by linear superposition of the symmetric and antisymmetric parts.

Calculated Results

The calculated results presented herein were obtained using the IBM 370/195 computer and the Douglas Aircraft Co. "Matrix Aeroelastic Loads System" (MALS)[10] The objective here is to show the effect of several recent state-of-the-art advances on the trimmed aeroelastic loads solution of two common aircraft configurations.

The two selected configurations are the Doublas DC-10-30 and AST Model 3230-2.2-5 airplanes. The DC-10-30 is representative of the wide-body commercial subsonic transports which are in use by the airlines today. The AST Model 3230-2.2-5 is a general representation of a possible future supersonic commercial transport. Figures 4 and 5 show the finite element aerodynamic and structural idealizations for these configurations. The DC-10-30's 278 aerodynamic degrees of freedom are typical of a production-type loads analysis and the 145 aerodynamic degrees of freedom used on the AST are indicative of a more preliminary investigation.

The method divides the aeroelastic trim solution into linear and nonlinear parts. The nonlinear trim parameters arise from the consideration of aerodynamic drag, and the squares and cross products of the angular velocities. These nonlinear terms are determined by successive iterations of the classical closed-form aeroelastic solution. In all cases investigated to date, this approach has assured a rapid closure of the iterative solution. Table 1 indicates the closure of unknown trim parameters on the DC-10-30 for a 2.5-g maneuver and a high cruise dynamic pressure.

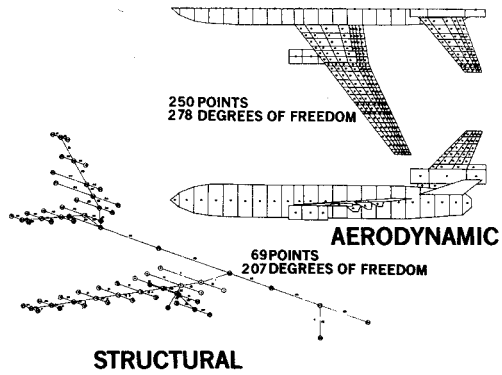

Fig.4 DC-10 finite element idealizations.

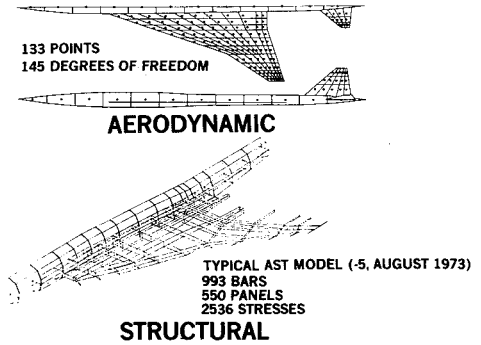

Fig. 5 AST finite element idealization.

Table 1 Closure of iterative solution - Model DC-10-30[a]

TRIM PARAMETER	RIGID ITERATION				ELASTIC ITERATION			
	1	2	3	4	1	2	3	4
α (RAD)	0.03799	0.03812	0.03812	0.03812	0.05364	0.05361	0.05360	0.05360
δ_t (RAD)	−0.00381	−0.00428	−0.00429	−0.00429	−0.01438	−0.01420	−0.01419	−0.01419
N_x	0.04926	0.07356	0.07321	0.07320	0.07320	0.04537	0.04551	0.04551

[a] M = 0.6; q = 3.707 psi; n_z = 2.5; GW = 335,000 lb

The use of finite element surface aerodynamic theory allows the inclusion of chordwise cambering in the aeroelastic solution. To accomplish this, it is necessary to find a transformation function [Z] which relates the displacements of the points on the structural grid to the displacements of the points on the aerodynamic grid [see Eq. (11)]. Double interpolations, parabolic series, and polynomial equations are some of the functions which have been proposed. The cumbersome bookkeeping, the ill-behavior, and the analytical restrictions of this group of functions make them difficult to handle. Indeed, many times the aeroelastician has simply forced his structural idealization to coincide with his aerodynamic idealization, thus avoiding the problem altogether. Of course, his structural idealization may have left a lot to be desired, but this sometimes seemed preferable to the interpolation problem.

Harder[9] proposed a surface spline function based on symmetrically loaded plates as a solution to this dilemma. The surface spline is extremely well behaved, easily cast in matrix form, and is analytical, thus allowing differentiation to obtain aerodynamic normalwash boundary conditions. SIC's and AIC's in rectangular matrix form, Eqs. (9) and (14), are simply determined by using the surface spline function. Once these rectangular influence coefficient matrices have been obtained, the classical closed-form static aeroelastic solution, Eq. (28), may be generated from independent aerodynamic and structural grid systems. An additional advantage derived from this approach is a reduction in the order of the aeroelastic inverse $[G]^{-1}$ required by Eq. (28) since the number of structural points necessary to define the vehicle distortion is normally less than the number of finite aerodynamic elements.

The effects of aeroelastic cambering of streamwise sections on low aspect ratio wings are generally known. However, chordwise cambering is generally neglected in aeroelastic calculations on high aspect ratio wings, but its existence can readily be shown. A panel is assumed to be oriented in the swept elastic axis coordinate system (ξ,η), as in Fig. 6.

Assume the panel is rigid in the ξ direction. Then the deflections are a function of η only. If a parabolic elastic axis deflection is assumed,

$$h = h_0 + a\eta + b\eta^2$$

where h_0, a, b are constants, and

$$\eta = y \cos \Lambda \; x \sin \Lambda$$

the streamwise slope of the panel, may now by calculated by differentiation.

$$\partial h/\partial x = (dh/d\eta)\,(\partial\eta/\partial x) =$$

$$a \sin \Lambda + 2b\, y \sin \Lambda \cos \Lambda + 2b\, x \sin^2 \Lambda$$

Therefore, the chordwise cambering on a high aspect wing is a function of the elastic axis sweep angle and the wing bending deflection

The influence of this chordwise flexibility on high aspect ratio swept wings is to further reduce the outboard wing span loading over that of a rigid chordwise $(\Delta\alpha_e)$ aeroelastic solution (Fig. 7). The DC-10-30 showed a change in wing span loading of up to 4% for typical design conditions when chordwise flexibility was considered (Figs. 8-10). Figure 9 indicates that, for a constant aerodynamic configuration, i.e., no

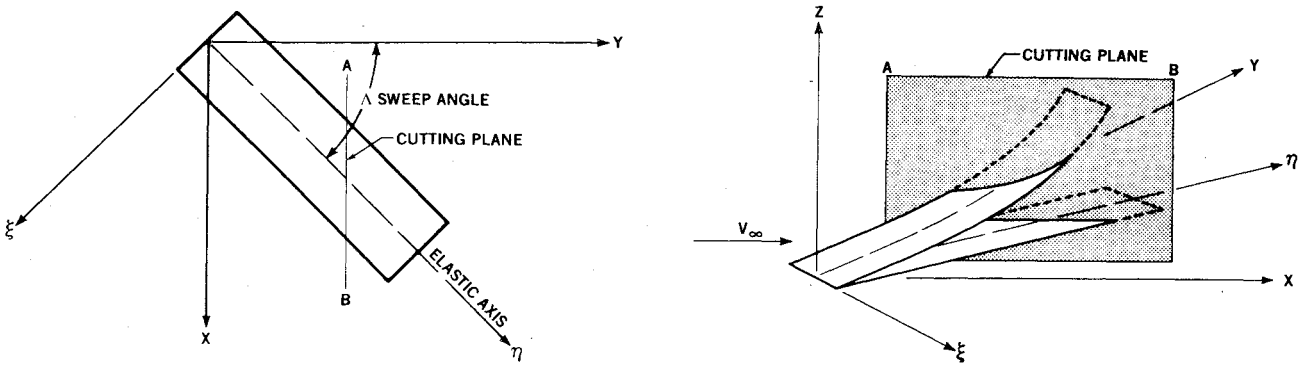

Fig. 6 Chordwise cambering of high-aspect ratio wing.

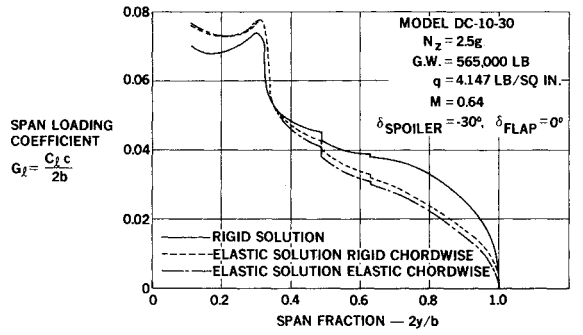

Fig. 7 Change in DC-10 wing span loading due to chordwise aeroelastic cambering.

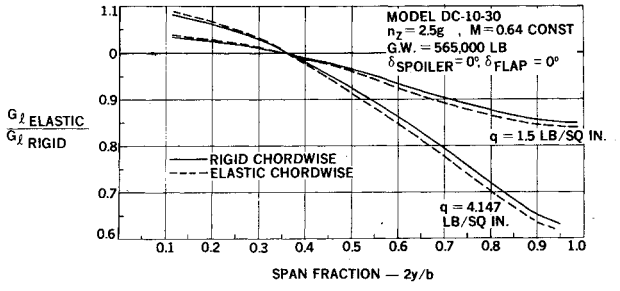

Fig. 8 DC-10 elastic to rigid span loading ratio.

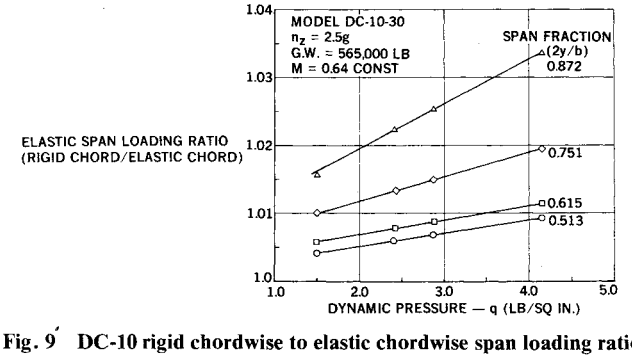

Fig. 9 DC-10 rigid chordwise to elastic chordwise span loading ratio vs q.

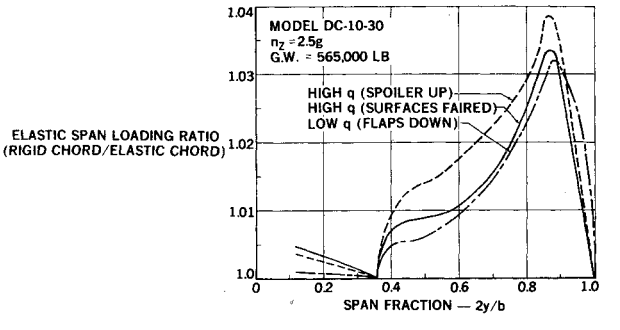

Fig. 10 DC-10 rigid chordwise to elastic chordwise span loading ratio vs span.

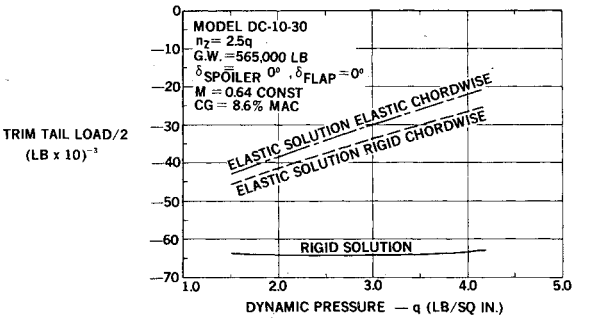

Fig. 11 DC-10 trim tail load vs q.

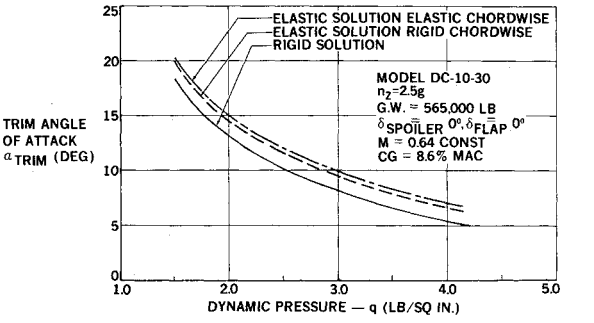

Fig. 12 DC-10 Trim Angle of Attack vs q.

change in control surface deflection, a near linear relationship exists between dynamic pressure and rigid chordwise to elastic chordwise span loading ratio at a given wing station.

The variation of this rigid chordwise to elastic chorwise span loading ratio with extreme changes in chordwise aerodynamic loading is shown in Fig. 10. It is obvious that, in addition to the previously suggested wing bending deflection and sweep angle parameters, wing torsion also has a considerable effect on the DC-10-30 chordwise flexibility ratio. For example, a ratio distribution similar to a high-speed, clean wing condition may be achieved at a low speed by deflecting the flaps. The change due to elastic chordwise cambering in the DC-10-30 trim tail load and angle of attack is shown in Figs. 11 and 12.

Conclusions

Increased structural and aerodynamic design synthesis and optimization now demand a refinement of static aeroelastic techniques. The method presented in this paper is one example of the new techniques[11,12] required to meet these design challenges.

Second-order effects, which were previously considered negligible, must now be included in the analysis. Chordwise aeroelastic cambering, aerodynamic interference of surfaces and bodies, and inertially coupled forces are some of the second-order effects which are handled by the present method.

Aerodynamic drag must be included in the equilibrium equations if an accurate trim solution is to be obtained. Since the calculation of the drag distribution requires the predetermination of the lift distribution, the classical closed-form aeroelastic solution is not directly applicable. If the entire static problem were to be approached from an iterative solution, a large number of cycles might be required for closure. Indeed, if divergence were present, an iterative closure would be impossible. Therefore, a combination linear and iterative solution was developed

The lifting problem is considered to be linear and a direct solution is formulated. Component divergence is easily predictable using this approach and the linear solutions are used as initial parameters for the nonlinear iteration. This technique ensures the rapid closure of the iterative series.

The matrix influence coefficient technique provides the additional advantage that the approach is unchanged for the purposes of preliminary design, design, or substantiation analyses. Only the complexity of the required aerodynamic and structural influence coefficients is varied.

References

[1] Hedman, S. C., "Vortex Lattice Method for Calculation of Quasi-Steady Loadings on Thin Elastic Wings in Subsonic Flow," Rept. 105, 1966, Federal Aviation Administration, Washington, D.C.

[2] Rodden, W. P. and Farkas, E. F., "Quasi-Static Aero-Thermo-Elastic Analysis," Rept. TDR-169 (3230-11) TN-8, March 1, 1963, Aerospace Corp., El Segundo, Calif.

[3] "An Analysis of Method for Predicting the Stability Characteristics of an Elastic Airplane," Summary Rep. NASA CR73277, Nov. 1968.

[4] Roskam, J., "Flight Dynamics of Rigid and Elastic Airplanes," 1972, Roskam Aviation and Engineering Corp., Lawrence, Kansas.

[5] Kemp, W. B., Jr., "Definition and Application of Longitudinal Stability Derivatives for Elastic Airplanes," NASA TN D-6629, 1972.

[6] Giesing, J. P., Kalman, T. P., and Rodden, W. P., "Application of the Doublet-Lattice Method and the Method of Images to Lifting-Surface/Body Interference," Rep. AFFDL-TR-71-5, Aug. 1971, Air Force Flight Dynamics Lab., Wright-Patterson Air Force Base, Ohio.

[7] James, R. M., "On the Remarkable Accuracy of the Vortex Lattice Discretization in Thin Wing Theory," Rept. DAC-67211, Feb. 1969, Douglas Aircraft Co., Long Beach, Calif.

[8] Stahl, B., Kalman, T. P., Giesing, J. P., and Rodden, W. P., "Aerodynamic Influence Coefficients for Oscillating Planar Lifting Surfaces by the Doublet-Lattice Method for Subsonic Flows including Quasi-Steady Fuselage Interference," Rept. DAC-67201, Oct. 1968, Douglas Aircraft Co., Long Beach, Calif.

[9] Harder, R. L. and Desmarais, R. N., "Interpolation Using Surface Splines," *Journal of Aircraft*, Vol. 9, Feb. 1972, pp. 189-191.

[10] Rowan, J. C. and Burns, T. A., "FORMAT - Engineering User and Technical Report - Matrix Aeroelastic Loads Systems (MALS)," Rept. DAC-33569, Vol. V, Supp. II, April 1973, Douglas Aircraft Co., Long Beach, Calif.

[11] Rowan, J. C. and Burns, T. A., "Matrix Solution for Loads, Deflections, and Trim Parameters for an Elastic Vehicle in Quasi-Static Aeroelastic Equilibrium," Rept. MDC-J1065, Dec. 1970, Douglas Aircraft Co., Long Beach, Calif.

[12] Rowan, J. C. and Burns, T. A., "Quasi-Static Aeroelasticity," Rep. MDC-J5550, Jan, 1972, Douglas Aircraft Co., Long Beach, Calif.